Ecosystems
https://doi.org/10.1007/s10021-019-00376-8

Carbon Dioxide and Methane Emissions from Peat Soil in an Undrained Tropical Peat Swamp Forest

Kiwamu Ishikura,[1,5]* Ryuichi Hirata,[2] Takashi Hirano,[1] Yosuke Okimoto,[1] Guan Xhuan Wong,[1,3] Lulie Melling,[3] Edward Baran Aeries,[3] Frankie Kiew,[1,3] Kim San Lo,[3] Kevin Kemudang Musin,[3] Joseph Wenceslaus Waili,[3] and Yoshiyuki Ishii[4]

[1]*Research Faculty of Agriculture, Hokkaido University, Kita-ku, Kita 9, Nishi 9, Sapporo, Hokkaido 060-8589, Japan;* [2]*Center for Global Environmental Research, National Institute for Environmental Studies, Tsukuba, Ibaraki 305-8506, Japan;* [3]*Sarawak Tropical Peat Research Institute, Lot 6035, Kuching – Kota Samarahan Expressway, 94300 Kota Samarahan, Sarawak, Malaysia;* [4]*Institute of Low Temperature Science, Hokkaido University, Kita-ku, Kita 19, Nishi 8, Sapporo, Hokkaido 060-0819, Japan;* [5]*Present Address: Production and Environment Group, Tokachi Agricultural Experiment Station, Hokkaido Research Organization, 9-2, Shinsei Minami, Memuro, Hokkaido 082-0081, Japan*

Abstract

This study investigates the factors controlling the soil CO_2 and CH_4 fluxes and quantifies annual cumulative soil respiration (R_S), heterotrophic respiration (R_H), and soil CH_4 emission in an undrained forest on tropical peat by continuous measurement using an automated chamber system for 2 years. Daily mean soil CO_2 flux was increased by lowering groundwater level (GWL), which indicates oxidative peat decomposition is promoted by the enhancement of aeration. On the other hand, soil CH_4 flux showed a bell-shaped relationship with GWL, which suggested that the development of anaerobic conditions promoted CH_4 production by the rise in GWL, whereas hydrostatic pressure suppressed CH_4 diffusion when the GWL was above the peat surface. Mean annual gap-filled CO_2 emissions were 926 ± 610 and 891 ± 476 g C m^{-2} y^{-1} (mean ± 1 SD) for R_S (n = 10) and R_H (n = 6), respectively, and were not significantly different from each other. The annual R_H in this study was similar to that of previous studies despite the higher annual mean GWL in this study, possibly due to the inclusion of litter decomposition in contrast to most of the previous studies in tropical peatland. Mean annual gap-filled CH_4 emission was 4.32 ± 3.95 g C m^{-2} y^{-1} (n = 9), which was the high end of the previous studies in tropical peatland due to higher annual mean GWL in this study. In conclusion, R_S was lower and CH_4 emission was higher in the undrained peat swamp forest than those previously reported for drained and disturbed forests on tropical peat.

Received 10 September 2018; accepted 22 March 2019

Electronic supplementary material: The online version of this article (https://doi.org/10.1007/s10021-019-00376-8) contains supplementary material, which is available to authorized users.

Authors Contribution RH, TH, YO, and LM designed the experiment; YI prepared the chambers; GXW collected the site information and meteorological data; RH, YO, GXW, LM, EBA, FK, KSL, KKM, and JWW performed the experiment; KI and RH analyzed the data; KI and TH wrote the manuscript; LM commented on details of the manuscript drafts.

**Corresponding author; e-mail:* ishikura-kiwamu@hro.or.jp

Published online: 10 April 2019

Key words: automated chamber system; groundwater level; heterotrophic respiration; methane flux; oxidative peat decomposition; soil respiration; trenching.

Highlights

- Soil CO_2 and CH_4 fluxes were continuously measured in undrained tropical peat forest.
- CO_2 flux was promoted by low GWL, and CH_4 flux was maximized at GWL near surface.
- CO_2 flux was lower and CH_4 was higher than previously reported in undrained forests.

Introduction

Carbon dioxide (CO_2) and methane (CH_4) are the most and second most important anthropogenic greenhouse gases, respectively, and CH_4 has a 28 times greater global warming potential than CO_2 over a 100-year time horizon (IPCC 2013). CH_4 emission from wetland including peatland has an important role in the global CH_4 budget with large spatiotemporal variations (IPCC 2013). Therefore, it is important to understand the factors controlling CO_2 and CH_4 fluxes in peatland to provide accurate estimates of annual emissions (Sjögersten and others 2014).

Peatland covers only 3% of the global terrestrial area, but it is an important carbon (C) reservoir because peatland has accumulated about one-third of global soil carbon stocks (Page and others 2011; Lawson and others 2014; Dargie and others 2017). The large C stocks in peatlands result from net C accumulation during the Holocene (Page and others 2004; Smith and others 2004; Yu and others 2010), and, in tropics, it is recognized that intact peatlands coexisting with swamp forests can function as contemporary C sinks (Kiew and others 2018). However, tropical peatlands have been reclaimed rapidly from natural forest to oil palm plantations, *Acacia* plantations, and smallholders' farmland in the last three decades (Miettinen and others 2017). This land-use change involves drainage which, in tropical peatland, results in the enhancement of CO_2 emission from peat surface and in the weak uptake of CH_4 (Inubushi and others 2003; Arai and others 2014), which has caused these ecosystems to change from net C sinks to net C sources (Dommain and others 2014; Miettinen and others 2017). Nevertheless, studies on CO_2 and CH_4 emissions are still limited in the undrained tropical peat swamp forest (Hirano and others 2009; Wright and others 2013; Teh and others 2017) compared with drained peat forest (Inubushi and others 2003; Hadi and others 2005; Murakami and others 2005; Jauhiainen and others 2008, 2014; Melling and others 2013; Sangok and others 2017). Thus, evaluating the scale of the CO_2 and CH_4 emissions from undrained pristine swamp forest on tropical peat is necessary to provide reference data sets to better quantify the impact of land-use change on C emissions.

Soil respiration (R_S) is measure of the total CO_2 emissions from the soil surface, which consists of heterotrophic respiration (R_H) and root respiration. In peatland ecosystems, oxidative peat decomposition dominates R_H, especially when the peatland is drained (Toma and others 2011; Jauhiainen and others 2012). Studies on R_S have been widely performed in tropical peatland by using the chamber method (Inubushi and others 2003; Melling and others 2005b; Murakami and others 2005; Jauhiainen and others 2008; Sundari and others 2012; Arai and others 2014; Comeau and others 2016; Ishikura and others 2017). On the other hand, R_H results from microbial decomposition of aboveground leaf litter, belowground root litter, and soil organic matter. Therefore, along with R_S, the measurement of R_H is important because R_H represents C loss from the peat soil. However, studies on R_H are still limited compared with R_S in tropical peatland (Hirano and others 2014; Jauhiainen and others 2014; Wakhid and others 2017; Ishikura and others 2018), especially in natural forests (Itoh and others 2017). Also, studies on soil CH_4 emissions are limited in tropical peatland compared with boreal peatland. In previous studies, soil CH_4 flux was mostly measured monthly for more than one year (Inubushi and others 2003; Furukawa and others 2005; Melling and others 2005a) or was measured at shorter intervals but for less than one year (Hadi and others 2005; Adji and others 2014) in tropical peatland using manual chamber systems. Ecosystem-scale CH_4 flux has been evaluated recently in tropical peatland by using eddy covariance method (Sakabe and others 2018; Wong and others 2018). However, factors controlling CH_4 flux are not understood well in tropical peatland yet, and the spatiotemporal variation of CH_4 flux is high (Sjögersten and others 2011).

Continuous measurement of soil CO_2 and CH_4 fluxes over one year can detect both diurnal and seasonal flux variations following environmental variations, which will contribute to an improved

understanding of environmental responses of soil CO_2 and CH_4 fluxes. Moreover, spatial evaluation may increase the accuracy of the soil CO_2 and CH_4 emissions. Therefore, we measured R_S, R_H and soil CH_4 fluxes continuously using an automated chamber system for 2 years in an undrained swamp forest on tropical peat. The objectives of this study are (1) to clarify the controlling factors of soil CO_2 and CH_4 fluxes and (2) to quantify annual soil CO_2 and CH_4 emissions in an undrained forest on tropical peat.

Materials and Methods

Site Description

The field study was conducted in an undrained swamp forest, which is classified as ''Alan Batu Forest'', in Maludam National Park (1°27′N, 111°9′E), Sarawak, Malaysia (Figure 1). Mean annual air temperature and precipitation between 1998 and 2016 were 26.6 ± 0.3 °C and 3161 ± 471 mm y^{-1} (mean ± 1 standard deviation (SD)), respectively, at Lingga meteorological station (Department of Irrigation and Drainage Sarawak) about 12 km away from the study site. Although the forest had been selectively logged, it has been conserved as a national park since 2000 (Melling 2016). An experimental area was established 4.5 km away from the Batang Lupar River and about 20 m away from an eddy flux tower. The dominant species is *Shorea albida* Sym., and aerial and buttress roots are well developed. Tree density was 1173 trees ha^{-1} (diameter at breast height (DBH) > 5 cm), and plant area index was 6.4 m^2 m^{-2}. The understory vegetation consisted of pitcher plant (*Nepenthes ampullaria* Jack), and herbs and shrubs (*Uraria crinita* (L.) Desv. ex DC., *Scleria sumatrensis* Retz, *Pandanus helicopus* Kurz, and *Aglaonema nitidum* (Jack) Kunth.). The forest floor shows microtopography, and the elevation differences are generally 30–40 cm between the top of hummock and the base of hollows. Hummocks are mainly overgrown with dense tree roots. The soil is classified as a Fibric Histosol (IUSS Working Group WRB 2015) with peat thickness of 10 m. Table 1 shows soil physicochemical properties in the experimental area.

Experimental Design and Chamber Measurement

Six trenched plots were established in the experimental area in November 2014 for measurement of R_H. Each plot was a square of 40 cm by 40 cm with stainless-steel plates inserted into a depth of 80 cm, which is deeper than the depth distribution of fine roots. Also, ten non-trenched plots were established for R_S. Two non-trenched plots and two trenched plots were set on hummocks, and the

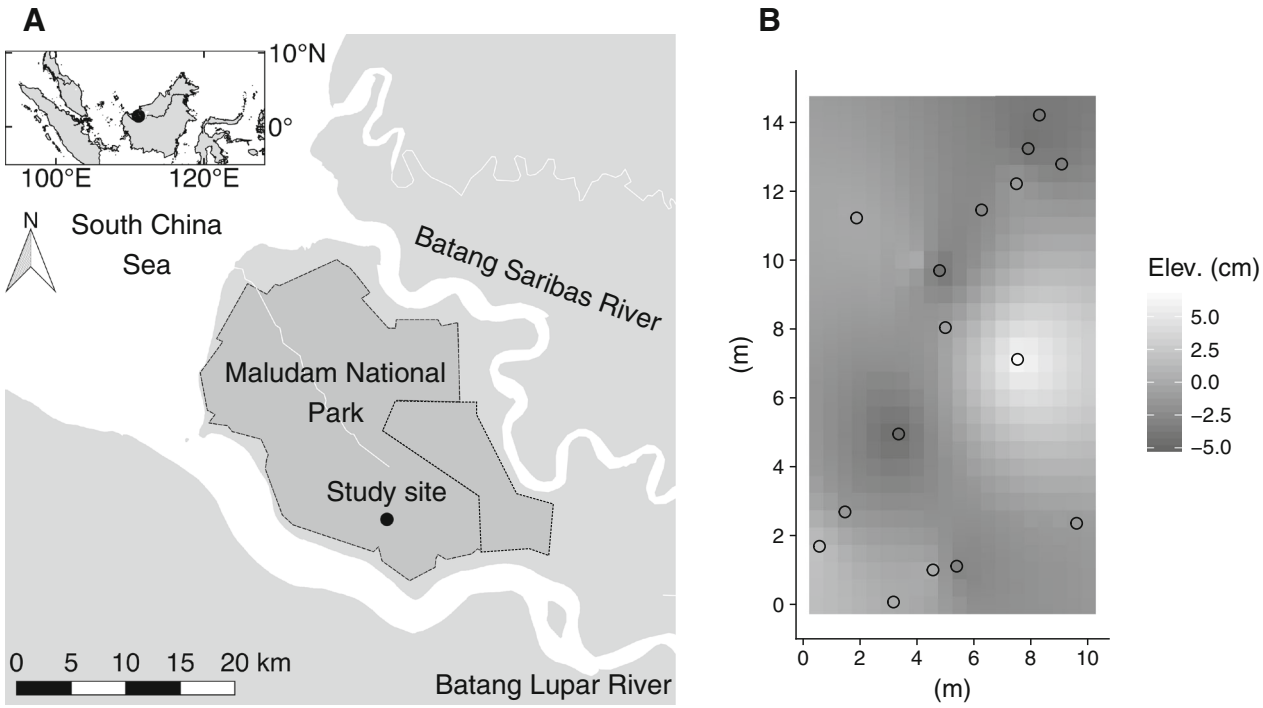

Figure 1. Map of the study site.

Table 1. Soil Physicochemical Properties in 0–30 cm Depth (0–10 cm Depth for Bulk Density)

Properties	Mean ± 1 SD (*n*)
Bulk density (Mg m^{-3})	0.10 ± 0.02 (11)
Total C (%)	52.5 (3)
Total N (%)	1.7 (3)
Ash content (%)	0.9 (3)
Soil pH (H_2O)	3.5 (3)
CEC ($cmol_C$ kg^{-1})	25.0 (3)
Base saturation (%)	69.6 (3)

CEC cation exchange capacity.

other plots were set in hollows. The understory vegetation was removed from these plots.

An automated chamber system was installed in August 2015, 9 months after trenching. The system consists of 16 chambers, a greenhouse gas analyzer (Ultraportable Greenhouse Gas Analyzer 915-0011, Los Gatos Research, Inc., San Jose, California, USA), a programmable data logger (CR1000, Campbell Scientific Inc., Logan, Utah, USA), and solenoid valves (Hirano and others 2009; Ishikura and others 2018). Chambers were made of an opaque polyvinyl chloride (PVC) cylinder with a height of 40 cm and an inner diameter of 25 cm. A chamber was inserted 2–3 cm deep into the soil. An opaque PVC lid attached to the chamber top opened and closed vertically under the control of the data logger. Each chamber closed for 225 s (s) one after another in an hourly rotation, and the headspace air of the closed chamber was pumped into the gas analyzer. CO_2, CH_4, and water vapor concentrations were measured at 10-s intervals and recorded in the data logger. Although the measurement began in August 2015, data from October 2015 to October 2017 was only used in this study, because the decomposition of cut roots by trenching left in the trenched plots was expected to influence soil CO_2 and CH_4 fluxes for several months after trenching (Hanson and others 2000; Comeau and others 2016).

Soil CO_2 and CH_4 fluxes (F; μmol m^{-2} s^{-1} for CO_2 or nmol m^{-2} s^{-1} for CH_4) were calculated from the rate of change in CO_2 or CH_4 concentration in each chamber headspace during 90–220 s after chamber closing in consideration of dilution by water vapor using the following equation (Jassal and others 2012; Harazono and others 2015):

$$F = \frac{PH}{RT_{\mathrm{air}}(1 - s_{\mathrm{W}})} \frac{\mathrm{d}s_{\mathrm{C}}}{\mathrm{d}t} \quad (1)$$

where P is the standard air pressure (101.325 kPa), H is the aboveground height of a chamber, R is the gas constant (8.314 Pa m^3 K^{-1} mol^{-1}), T_{air} is air temperature (K), ds_c/dt is the rate of change in CO_2 or CH_4 mixing ratio [μmol CO_2 (mol dry air)$^{-1}$ s^{-1} or nmol CH_4 (mol dry air)$^{-1}$ s^{-1}], and s_w is water vapor mixing ratio [mol H_2O (mol dry air)$^{-1}$], respectively. Mixing ratio was calculated from gas concentration (c; μmol CO_2 mol^{-1} or nmol CH_4 mol^{-1}) and water vapor concentration (w; mol H_2O mol^{-1}) as follows: $s_C = c/(1 - w)$ and $s_W = w/(1 - w)$. The ds_C/dt was determined by the least-squares method.

The quality of flux data was controlled as follows:

1. Significant slope: Pearson's correlation coefficient of the rates of change in mixing ratio (ds_C/dt) should be higher than 0.661376 ($P < 0.01$, $n = 14$);
2. Stationarity: the rates of change in mixing ratio from 90 to 150 s and 160 to 220 s after lid closure were calculated separately. The difference between the mean of the two rates and the rate for the whole period (90–220 s) should be less than 30% (Aguilos and others 2013);
3. Initial concentration: initial concentrations should be between 350 and 1000 μmol mol^{-1} for CO_2 and 1600 and 3000 nmol mol^{-1} for CH_4, respectively.
4. Outlier removal: boxplot outliers on each date were removed using a 15-days moving window.

In total, 26% of data were missed in this study period mainly because of power problems and malfunction of the gas analyzer. After the quality control, 55 and 45% of data were finally available for CO_2 and CH_4 fluxes, respectively (Table S1). Soil CO_2 fluxes from the non-trenched and trenched plots correspond to R_S ($n = 10$) and R_H ($n = 6$), respectively. Soil CH_4 flux was calculated for both non-trenched and trenched plots. Because litter fall accumulated in all chambers, the CO_2 and CH_4 emissions through litter decomposition were included in R_S, R_H, and soil CH_4 emissions, respectively, though the amount of litter fall was not measured in this study.

Environmental Properties

Precipitation was measured at a height of 1 m in an open space about 20 m away from the experimental area. Precipitation data at Lingga meteorological station was alternatively used to fill missing data due to power failure. Friction velocity (u^*, m s^{-1}) was measured at a height of 41 m above the forest canopy using a sonic anemometer (CSAT3,

Campbell Scientific Inc.) (Wong and others 2018). Here, we assumed that the atmospheric turbulence near the soil surface is linked to that above the canopy. Thus, the $u*$ was used as an index of the atmospheric turbulence near the soil surface.

Air and soil temperatures (5 cm depth) were measured in the same two chambers in the non-trenched plots using handmade thermocouple thermometers (type T). Groundwater level (GWL, m) was measured at a hollow using a piezometer (HTV-050KP, Sensez, Tokyo, Japan), which is shown as the distance between ground and water surfaces with positive values representing flooding. Half-hourly means of these variables were recorded to the same data logger as for the chamber system. Missing GWL data were gap-filled from precipitation on a daily basis using a tank model (He and Inoue 2015). The elevation difference between the GWL measurement position and each plot was surveyed. GWL at each plot was determined (GWL_p) using the elevation difference. If GWL_p was positive, H in Eq. (1) was corrected as $H - GWL_p$.

Undisturbed soil cores (100 cm^3) were taken from 0 to 10 cm depth every month with a stainless-steel soil core cylinder, and bulk density (Mg m^{-3}) was determined by measuring the oven-dried weight of the cores for more than 48 h at 105 °C. Disturbed soil samples (0–10 cm depth) were taken in October 2012 in three replications, and sieved through 2-mm meshes after air-drying. Total C and nitrogen (N) contents (%) were analyzed by the dry combustion method (TruMac CN, LECO Corporation, St. Joseph, Michigan, USA). Ash content (%) was analyzed by loss-on-ignition (TGA701, LECO Corporation) at 800 °C for more than 1 h. Soil pH (1:2.5 H_2O) was measured using a digital pH meter (827 pH Lab, Metrohm AG, Herisau, Switzerland). Cation exchange capacity (CEC) and exchangeable cations (Na^+, K^+, Mg^{2+}, and Ca^{2+}) were determined by semi-micro Schollenberger's percolation method (Kamewada 1997) using a steam distillation method for NH_4^+ and using an inductively coupled plasma optical emission spectrometer (ICP-OES; Optima 7300 DV, PerkinElmer, Waltham, Massachusetts, USA) for base cations, respectively. Base saturation was calculated as the sum of the exchangeable cations divided by the CEC.

Data Analysis

We applied nonlinear mixed-effects modeling (lme4 package of R software; Bates and others 2015) to examine the dependencies of log-transformed daily mean soil CO_2 flux was fitted by the following bi-logistic equation for each of the non-trenched and trenched plots:

$$\ln(CO_2\,\text{flux}) = \frac{a_{1p}}{1+\exp\left[b_1\cdot\left(GWL_p - c_{1p}\right)\right]} + \frac{a_{2p}}{1+\exp\left[b_2\cdot\left(GWL_p - c_{2p}\right)\right]} + d_p \quad (2)$$

where GWL_p is the explanatory variable, a_{1p}, a_{2p}, b_1, b_2, c_{1p}, c_{2p}, and d_p are regression coefficients of pth plot (p = 1–16), respectively. The regression coefficients a_{1p}, a_{2p}, c_{1p}, c_{2p}, and d_p were described as follows:

$$a_{1p} = \overline{a_1} + \varepsilon_{a1p}, a_{2p} = \overline{a_2} + \varepsilon_{a2p}, c_{1p} = \overline{c_1} + \varepsilon_{c1p}, c_{2p} = \overline{c_2} + \varepsilon_{c2p}, d_p = \bar{d} + \varepsilon_{dp}$$

where $\overline{a_1}$,$\overline{a_2}$, $\overline{c_1}$, $\overline{c_2}$, and $\bar{d}$ are the fixed-effect coefficients (average coefficients among plots) and ϵ_{a1p}, ϵ_{a2p}, ϵ_{c1p}, ϵ_{c2p}, and ϵ_{dp} are the random-effect coefficients, respectively.

Daily mean soil CH_4 flux was fitted by GWL using the following Gaussian equation:

$$CH_4\,\text{flux} = a_{3p}\cdot\exp\left[b_3\cdot\left(GWL_p - c_{3p}\right)^2\right] \quad (3)$$

where GWL_p is the explanatory variable, a_{3p}, b_3, and c_{3p} are regression coefficients of pth plot, respectively. The regression coefficients a_{3p} and c_{3p} were described as follows:

$$a_{3p} = \overline{a_3} + \varepsilon_{a3p}, c_{3p} = \overline{c_3} + \varepsilon_{c3p}$$

where $\overline{a_3}$, and $\overline{c_3}$ are the fixed-effect coefficients, and ϵ_{a3p} and ϵ_{c3p} are the random-effect coefficients, respectively. These regression coefficients of Eqs. 2 and 3 were fitted by the residual maximum likelihood (REML) estimation method, and the goodness-of-fit was evaluated with the coefficient of determination (R^2).

The daily mean soil CO_2 and CH_4 fluxes were gap-filled using the regression equations (Eqs. 2 and 3, respectively), and the daily fluxes were summed up to annual emissions for each chamber from October 2015 to September 2016 (2015/16) and October 2016 to September 2017 (2016/17), respectively.

To evaluate the spatial average of annual emissions, soil CO_2 and CH_4 emissions were spatially interpolated as follows. Firstly, the experimental area was gridded at 50-cm, and spatial dependence of relative elevation was modeled using variograms fitted to a linear model. The relative elevation was spatially interpolated by ordinary kriging method. Secondly, nonlinear regression analysis of the 2-years mean annual R_S, R_H, and CH_4 emissions were

evaluated using relative elevation at each chamber position. Lastly, annual R_S, R_H, and CH_4 emissions were interpolated at each grid by using the regression equations of relative elevation. All the data analyses were conducted using R software (R Core Team 2017).

Results

Environmental Properties

This study site, even though it is relatively flat, has a peat surface microtopography (hollows and hummocks) with a relative elevation distance of between −4.5 and 6.5 cm at the chamber positions (Figure 1B). The soils showed the typical characteristics of ombrotrophic tropical peatland with low bulk density, high total C content, and acid soil pH (Table 1). Also, a high soil C/N ratio and low CEC suggest a low degree of peat decomposition at the study site.

The dry season is typically from May to August, and the rainy season is from October to February in this region (Chang and others 2005). However, precipitation was lower than the average from October 2016 to February 2017 (Figure 2A), which resulted in lower annual precipitation in 2016/17 (2524 mm y^{-1}) than in 2015/16 (3088 mm y^{-1}). Daily mean GWL varied between − 0.19 m in September 2015 and 0.25 m in January 2016 (Figure 2B) with annual means of 0.01 in 2015/16 and of − 0.01 m in 2016/17. Non-flooding periods were longer in 2016/17 than in 2015/16 because of less precipitation in 2016/17. Daily mean soil temperature varied between 25.4 and 28.0 °C without clear seasonal change (Figure 2C).

Diurnal Change of Soil Carbon Dioxide and Methane Fluxes

Both air and soil temperatures in the chambers showed a diurnal change (Figure 3A). The air temperature was at a minimum at 7 h and at a maximum at 14 h. Soil temperature showed a minimum at 10 h and a maximum at 20 h, which were delayed by 3–4 h from those of air temperature. The soil temperature was higher than the air temperature in the nighttime by 1.9 °C on average. The u^* above the canopy was also higher in the daytime than in the nighttime. In contrast, soil CO_2 and CH_4 fluxes were higher in the nighttime (Figure 3B).

To investigate the effect of moisture, temperature, and atmospheric turbulence on the diurnal change in soil CO_2 and CH_4 fluxes, standard least-squares multiple regressions were carried out without stepwise selection for hourly soil CO_2 and CH_4 fluxes, respectively, with predictors of GWL, soil temperature, $\Delta T_{\text{air-soil}}$ (the difference between air and soil temperatures), and u^*. All the predictors were significant for soil CO_2 fluxes both in the non-trenched and trenched plots (Table 2). GWL showed the greatest standardized coefficient for both plots, followed by $\Delta T_{\text{air-soil}}$. On the other hand, R^2 value was low for the regression model of soil CH_4 fluxes though all the predictors were significant due to the large sample sizes. GWL showed the greatest standardized coefficient for soil CH_4 fluxes as well as CO_2 fluxes. Because the diurnal change in GWL was not expected, and the diurnal range of soil temperature was small (Figure 3A), hourly soil CO_2 and CH_4 fluxes were plotted against $\Delta T_{\text{air-soil}}$ or u^* (Figure 4). Both CO_2 and CH_4 fluxes decreased as $\Delta T_{\text{air-soil}}$ increased when air temperature was higher than soil temperature (that is, $\Delta T_{\text{air-soil}} < 0$ °C). Similarly, both fluxes decreased as u^* increased.

Seasonal Change of Soil Carbon Dioxide and Methane Fluxes

To exclude biases derived from the diurnal change (Figure 3), daily mean soil CO_2 and CH_4 fluxes were calculated only when the number of available data was larger than six both in the daytime (7–18 h) and nighttime (19–6 h) on each day. The daily mean R_S and R_H were lower in the rainy season and higher in the dry season (Figures 5A, B). In contrast, the daily mean soil CH_4 flux was higher in the rainy season and lower in the dry season (Figure 5C). In November 2015, R_S and R_H increased (Figures 5A, B) just after the drastic rise in GWL from −0.17 m to +0.19 m (Figure 2B). Excluding high CO_2 fluxes in November 2015, Eq. 2 was significantly fitted to R_S and R_H with GWL_p (Figure 5A, B).

$$\ln(R_S) = \frac{3.61}{1+\exp\left(30.7\times\left(GWL_p-0.001\right)\right)} + \frac{0.33}{1+\exp\left(103\times\left(GWL_p+0.06\right)\right)} - 1.34 \quad \left(R^2=0.85, P<0.001\right)$$

$$\ln(R_H) = \frac{3.04}{1+\exp\left(53.3\times\left(GWL_p+0.012\right)\right)} + \frac{2.36}{1+\exp\left(84.9\times\left(GWL_p+0.08\right)\right)} - 1.27 \quad \left(R^2=0.88, P<0.001\right)$$

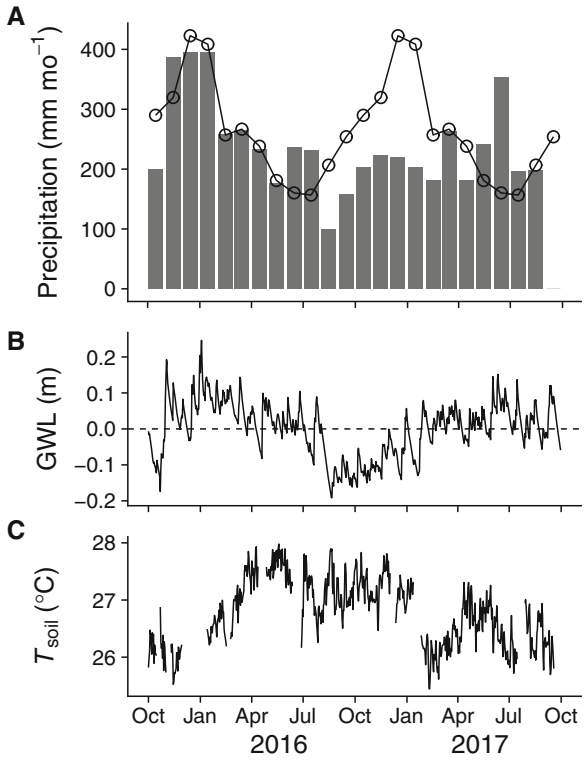

Figure 2. Seasonal changes in **A** monthly precipitation **B** daily mean GWL (groundwater level), and **C** daily mean T_{soil} (soil temperature) at 5 cm depth from October 2015 to September 2017. Precipitation data were from Lingga station. A line and open circles in **A** denote the means from 1998 to 2016.

This result showed that soil CO_2 flux increased as GWL_p lowered (Figure 6A, B). The daily mean R_S and R_H were similar to each other when GWL was lower than −0.1 m (Figure 6A), whereas R_S was higher than R_H when GWL was higher than −0.1 m (Figure 6B), which was the typical range of GWL in this site. Also, Eq. (3) was significantly fitted to daily mean soil CH_4 flux with GWL_p.

$$CH_4 = 13.5 \times \exp\left(-67.2 \times \left(GWL_p - 0.05\right)^2\right) \quad \left(R^2 = 0.48, P<0.001\right)$$

The result indicates that soil CH_4 flux was the maximum when the GWL was + 0.05 m (Figure 6C). The fitting parameters shown above are fixed-effects coefficients so that these equations represent the average relationships with GWL. Random-effects coefficients of each plot, which represent the deviation from the fixed-effects coefficient, are also calculated but not shown for simplicity.

R_H/R_S ratio showed a clear seasonal variation (Figure 7). The mean ratio in the rainy season was

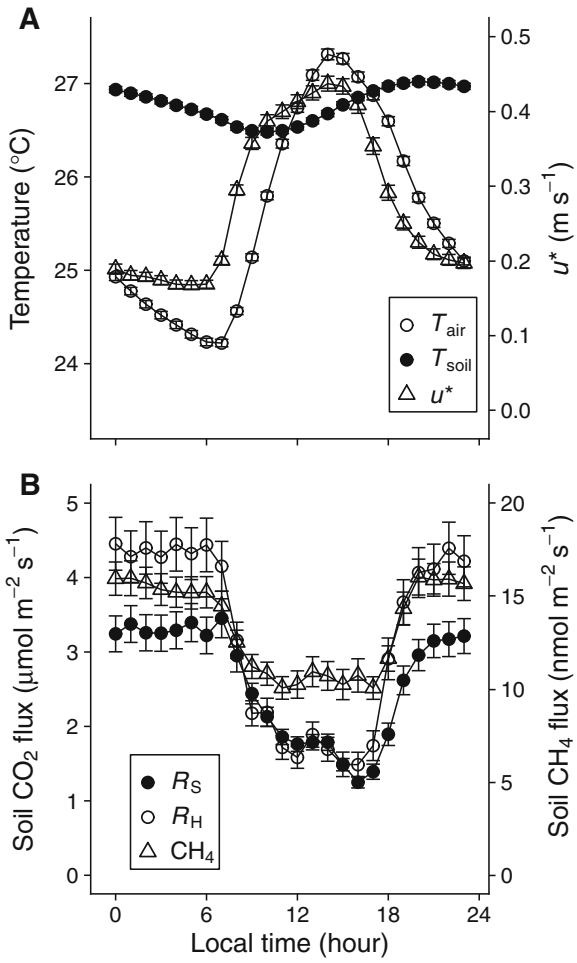

Figure 3. Ensemble-mean diurnal changes in **A** T_{air} (air temperature), T_{soil} (soil temperature), and u^* (friction velocity); and **B** R_S (soil respiration), R_H (heterotrophic respiration), and CH_4 fluxes. Error bars denote 95% confidence interval.

61%, whereas the mean ratio in the dry season was high, especially from August to November in 2016 when the ratio was higher than 100% (Figure 7).

Annual Soil Carbon Dioxide and Methane Emissions

Daily mean soil CO_2 and CH_4 fluxes were gap-filled for each plot from daily mean GWL_p using the regression models (Eqs. 2 and 3, respectively), and annual cumulative emissions were calculated for each chamber. The annual CO_2 emission was significantly fitted by a bell-shaped equation using relative elevation for both non-trenched and trenched plots (Figure 8A). Also, log-transformed CH_4 emission showed a significant negative correlation with relative elevation (Figure 8B). Annual soil CO_2 emission was slightly larger in the non-trenched (926 g C m^{-2} y^{-1}) than in the trenched plots

Table 2. Multiple Regression Analysis for Soil CO_2 (μmol m^{-2} s^{-1}) and CH_4 (nmol m^{-2} s^{-1}) Fluxes Using GWL (Groundwater Level, m), Soil Temperature (°C) at a Depth of 5 cm, $\Delta T_{air\text{-}soil}$ (Difference Between Air and Soil Temperature, °C), and u^* (Friction Velocity, m s^{-1})

	Predictor	Coefficient	Std. coeff.	*P* value	R^2
$\ln(R_S)$ (n = 66,746)	Intercept	− 2.68		< 0.001	0.49
	GWL	− 11.4	0.64	< 0.001	
	Soil temperature	0.089	0.04	< 0.001	
	$\Delta T_{air\text{-}soil}$	− 0.19	0.19	< 0.001	
	u^*	− 0.23	0.03	< 0.001	
$\ln(R_H)$ (n = 39,221)	Intercept	− 4.03		< 0.001	0.64
	GWL	− 15.8	0.75	< 0.001	
	Soil temperature	0.115	0.05	< 0.001	
	$\Delta T_{air\text{-}soil}$	− 0.27	0.21	< 0.001	
	u^*	− 0.11	0.01	< 0.001	
CH_4 flux (n = 86,088)	Intercept	− 76.1		< 0.001	0.03
	GWL	43.4	0.14	< 0.001	
	Soil temperature	3.29	0.09	< 0.001	
	$\Delta T_{air\text{-}soil}$	− 0.95	0.06	< 0.001	
	u^*	− 3.05	0.02	< 0.001	

R_S: soil respiration (CO_2 flux in the non-trenched (NTR) plots).
R_H: heterotrophic respiration (CO_2 flux in the trenched (TR) plots).
'Std. coeff.' represents the standardized regression coefficient. R^2 shows the coefficient of determination of the regression model.

(891 g C m^{-2} y^{-1}), though it was not significant, even if the outlier of the highest relative elevation (Figure 8A) was excluded (Table 3). Likewise, its interannual variation was not significant. Annual soil CH_4 emission was larger in the non-trenched (3.92 g C m^{-2} y^{-1}) than in the trenched plots (2.80 g C m^{-2} y^{-1}), which was not significant because of its large spatial variation (SD). Also, its interannual variation was not significant (Table 3).

Soil CO_2 (R_S and R_H) and CH_4 emissions were spatially interpolated (Figure 9) by kriged relative elevation (Figure 1B). R_H was estimated by using regression equation for R_S when relative elevation was higher than 1.84 cm because there was no measurement in higher relative elevation. Spatial means of R_S and R_H were slightly higher than simple means (Table 3). Even if the interpolated CO_2 emissions in higher relative elevation (> 1.84 cm) were excluded, the spatial means of R_S (1096 g C m^{-2} y^{-1}) and R_H (881 g C m^{-2} y^{-1}) were changed only 1.4–4.2% from the whole spatial means. On the other hand, spatial mean of CH_4 emission was 32% lower than simple mean (Table 3).

Discussion

Factors Controlling Soil Carbon Dioxide and Methane Fluxes

Diurnal Changes

Soil CO_2 and CH_4 fluxes decreased in the daytime and increased in the nighttime (Figure 3B), and hourly soil CO_2 and CH_4 fluxes were significantly increased as $\Delta T_{air\text{-}soil}$ and u^* decreased (Table 2, Figure 4). These negative relationships were also found in an oil palm plantation on tropical peat (Ishikura and others 2018). In the negative $\Delta T_{air\text{-}soil}$ conditions ($T_{air} < T_{soil}$) during the nighttime, soil CO_2 and CH_4 effluxes could have been enhanced by thermal convection in the porous soils (Ganot and others 2014). In addition, atmospheric turbulence can decrease diffusive CO_2 and CH_4 effluxes in the chambers (Lai and others 2012; Görres and others 2016). Moreover, CH_4 might have been rapidly oxidized in windy conditions even during flooding, because oxygen would be supplied into the surface water by wind (Poindexter and Variano 2013). However, the effect of atmospheric turbulence (u^*) on soil CO_2 and CH_4 fluxes by the closed chamber method was estimated to be 2–6%, which was much smaller than the difference of fluxes between the daytime and nighttime (Table S2).

Thus, the underestimation by the atmospheric turbulence might be negligible.

Soil CO_2 and CH_4 fluxes usually increase with soil temperature. However, the effect of soil temperature at 5 cm depth on soil CO_2 and CH_4 fluxes were not clear compared with other environmental variables (Table 2). In this study, hourly fluxes were higher in the nighttime when the soil temperature was lower than in the daytime. Therefore, the positive effect of soil temperature itself on fluxes would have been masked by the nighttime thermal convection.

Seasonal Change

Daily mean soil CO_2 efflux increased as GWL lowered (Figure 6A, B) like in previous studies (Inubushi and others 2003; Melling and others 2005b; Hirano and others 2009; Sundari and others 2012; Arai and others 2014; Ishikura and others 2017). Lower GWL enhances soil aeration, which promotes oxidative peat decomposition and gas diffusion in the soil. However, high soil CO_2 fluxes were found in November 2015 (Figure 5) just after the rapid rise in GWL from − 0.04 to + 0.19 m over 4 days (Figure 2B). The high CO_2 flux might be due to a ''rewetting effect'' (Birch 1958; Ishikura and others 2017), resulting from the following phenomena: (1) soil microbes killed during GWL drawdown were easily decomposed during subsequent rewetting (Marumoto and others 1977; Fraser and others 2016), (2) soil microbial activity is enhanced by the rewetting despite the unchanging population size (Placella and others 2012; Fraser and others 2016), and (3) the rise in GWL and soil moisture can physically displace CO_2 that accumulated in soil air during the dry period (Huxman and others 2004). The rewetting effect can continue for from a few hours to a few weeks (Borken and Matzner 2009; Bowling and others 2011). The high CO_2 fluxes lasted for 15 days in this study.

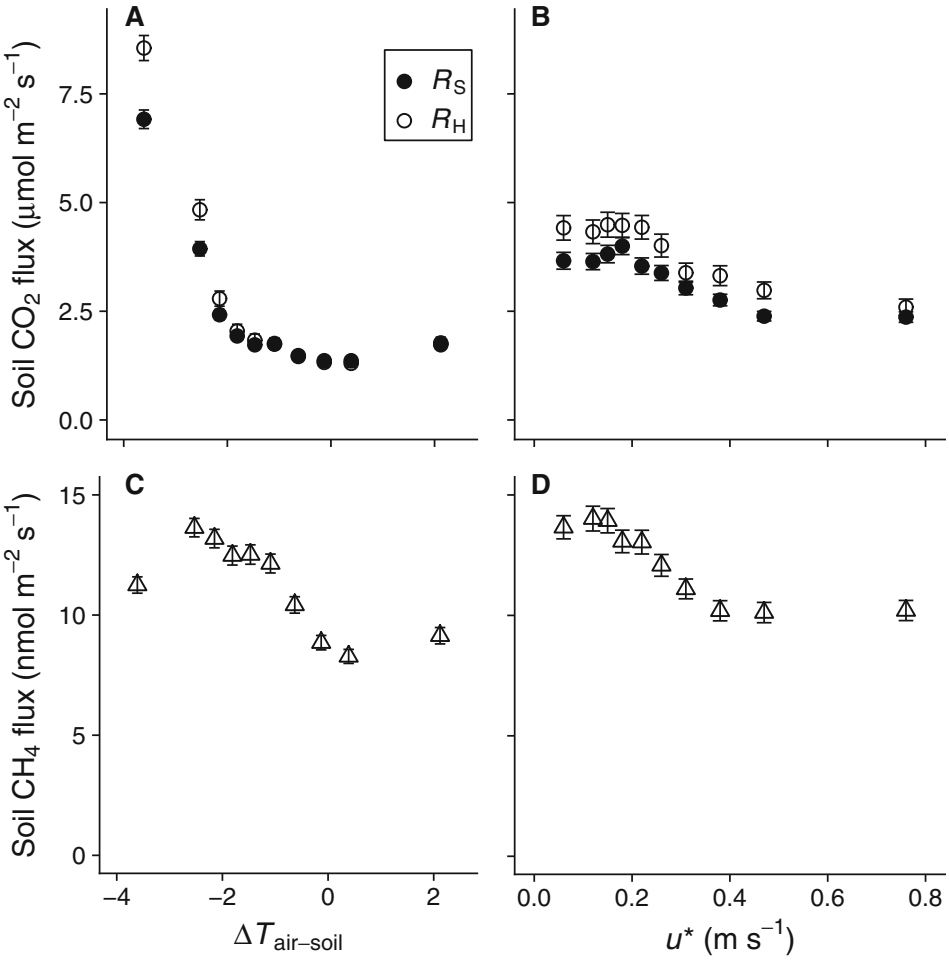

Figure 4. Relationship of soil CO_2 and CH_4 fluxes with $\Delta T_{air\text{-}soil}$ (difference of air and soil temperature) and u^* (friction velocity). Flux data were binned into deciles by $\Delta T_{air\text{-}soil}$ or u^*.

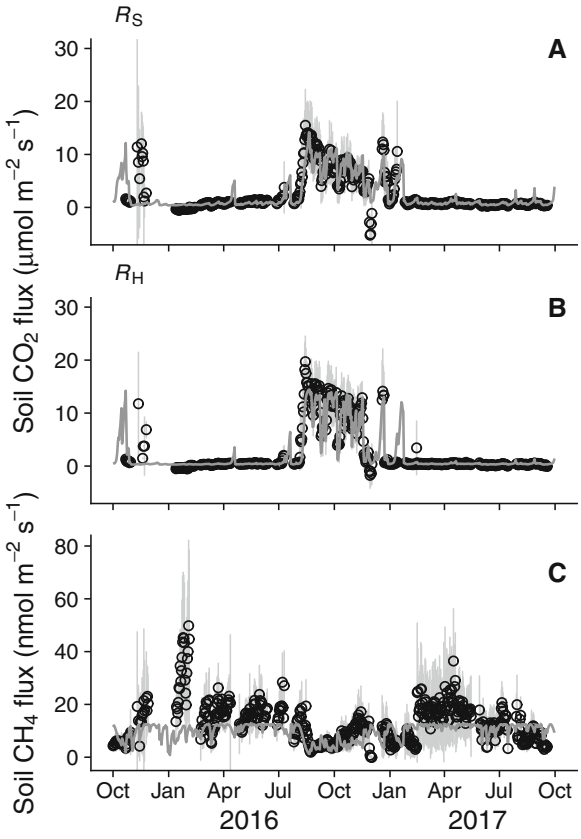

Figure 5. Seasonal change in daily mean soil CO_2 and CH_4 fluxes. R_S and R_H represent soil and heterotrophic respiration, respectively. Open circles and error bars show mean and 95% confidence interval of measured fluxes, and thick gray lines show predicted fluxes from groundwater level at each plot (GWL_p) using fitted equations (Eqs. 2 and 3), respectively.

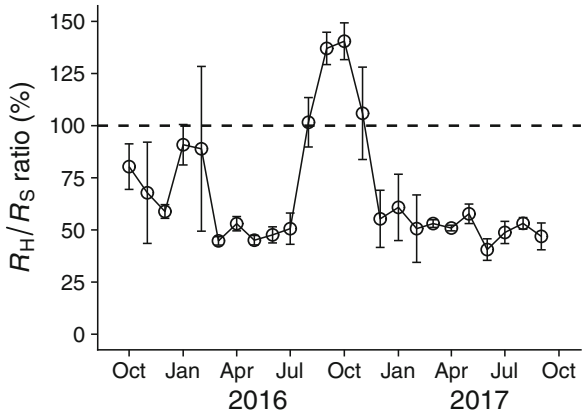

Figure 7. Seasonal change in monthly mean R_H/R_S (heterotrophic-to-soil respiration ratio, mean ± 95% confidence interval).

Soil CH_4 flux showed a bell-shaped relationship with GWL and peaked at 0.05 m (Figure 6C). Higher GWL promoted CH_4 production and suppressed CH_4 oxidation through thickening the soil anaerobic layer (Dise and others 1993; Jauhiainen and others 2008; Olefeldt and others 2013; Susilawati and others 2016). However, if GWL rose above 0.05 m, CH_4 efflux decreased with flooding depth. The decrease of CH_4 efflux was found in studies of paddy field (Yagi and others 1996; Minamikawa and Sakai 2006) and boreal peatland (Pelletier and others 2007; Turetsky and others 2014), because gas diffusion is restricted more as hydrostatic pressure increases along with increasing flooding depth. Furthermore, the standing water can enhance CH_4 oxidation because it would increase dissolved oxygen and prolong traveling time of CH_4 to the atmosphere (Strack and others 2004). The microbiological control on CH_4 pro-

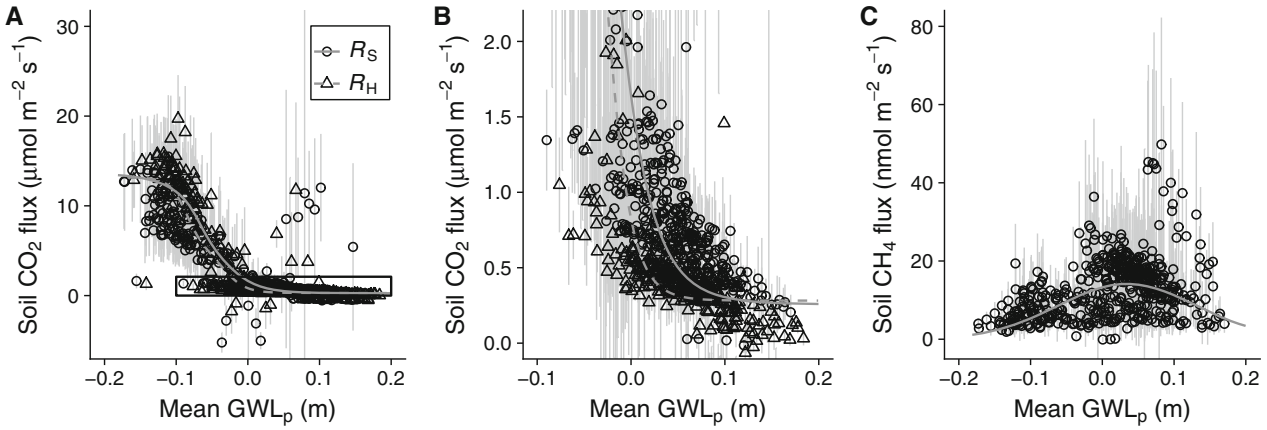

Figure 6. Relationships between **A** daily mean soil CO_2 flux and mean GWL_p (groundwater level at each plot); **B** the magnification of the box in **A**; and **C** daily mean soil CH_4 flux and GWL_p. R_S and R_H represent soil and heterotrophic respiration, respectively. Error bars show 95% confidence interval of measured fluxes.

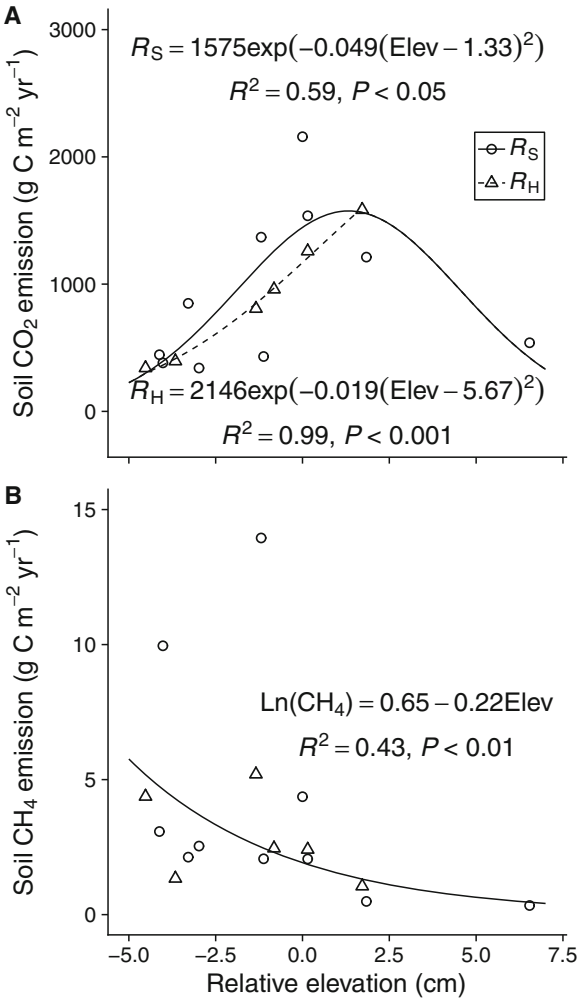

Figure 8. Relationship of 2-years mean annual soil **A** CO_2 and **B** CH_4 emissions with relative elevation. Circles with a solid line represent R_S (soil respiration) and open triangles with a dashed line represent R_H (heterotrophic respiration), respectively.

duction/oxidation and physical control on CH_4 diffusion result in the bell-shaped relationship between soil CH_4 efflux and GWL.

Annual Cumulative Emissions

Soil Carbon Dioxide Emission

The annual soil CO_2 emissions were not significantly different between R_S and R_H in this study (Table 3). Although the significant difference was not found between R_S and R_H, the R_H/R_S ratio was greater than 100% from July through December 2016 (Figure 7). The higher R_H than R_S is one of the largest concerns of the trenching method due to the additional CO_2 emission through the oxidative decomposition of dead roots remaining in the trenched plots. To exclude the additional CO_2 emissions, the trenching was made one year prior to the start of the measurement. Some studies have applied the trenching method to separate R_H from R_S in several land uses on tropical peat (Comeau and others 2016; Itoh and others 2017; Wakhid and others 2017; Ishikura and others 2018). In these studies, the measurement of soil CO_2 flux started 5–8 months after the trenching, and the trenched plots experienced lower GWL than − 0.5 m before the measurement. The low GWL might have caused the dead roots to undergo considerable decomposition before the measurement started. However, in this study, GWL remained high at above − 0.2 m after trenching. The higher GWL probably restrained the oxidative decomposition of dead roots, and the decomposition could have continued even during the measurement. As a result, R_H might be overestimated in this study.

Annual R_S and R_H are significantly fitted by a bell-shaped equation using relative elevation (Figure 8A). This result suggests that soil CO_2 emission was promoted by drier conditions up to 1.3 cm of relative elevation. The higher soil CO_2 emission in hummocks than in hollows has also been reported in other tropical peat forests (Hirano and others 2009; Sundari and others 2012). However, the exceptionally low outlier was measured at the highest position on a hummock (Figure 8A), which would increase the uncertainty of the bell-shaped relationship in higher relative elevation. Generally, soil bulk density is lower in hummocks than in hollows in tropical peat swamp forest (Lampela and others 2014) because of a vacant zone and root development in peat soils (Melling 2016). Thus, the amount of unsaturated peat soil might be smaller at the chamber position, resulting in the lower CO_2 emission. Moreover, lateral gas diffusion might not be negligible in a vacant zone in peat soils.

Soil Methane Emission

Annual CH_4 emission from the peat surface (non-trenched plots) was 3.92 ± 3.94 g C m^{-2} y^{-1}, and it increased to 4.32 ± 3.95 g C m^{-2} y^{-1} without the outlier (Table 3). Aerial roots of tree species living in tropical peat swamp forest can provide oxygen to the upper peat layer and enhance CH_4 oxidation (Pangala and others 2013; Adji and others 2014). In addition, the insufficient decomposition of dead roots in the trenched plots could provide substrates for CH_4 production. For these reasons, soil CH_4 emission is expected to be higher in the trenched plots, where no living roots exist. However, the CH_4 emission was unexpectedly lower in the trenched plots than in the non-tren-

ched plots (Table 3), possibly due to the enhancement of CH_4 production by root exudates (Girkin and others 2018) and imperceptible gaps between the peat and the stainless plates used for trenching. In this study, relatively small trenching plots of 0.4 m × 0.4 m were set. Oxygen might have been supplied into the peat through the gaps, and consequently, the peat might have been aerated in some trenched plots. Also, CH_4 produced in the peat might have leaked to the atmosphere through the gaps. Both the peat aeration and leakage potentially decrease the soil CH_4 emission. Similarly, soil CO_2 emission might have also been affected by the gaps.

Soil CH_4 emission was significantly promoted by wetter conditions (Figure 8B). The higher CH_4 emission in hollows than in hummocks has also been reported in other tropical peat forests (Jauhiainen and others 2008; Hirano and others 2009). The simple mean of CH_4 emissions was higher than the spatial mean (Table 3) probably because of the bias of the number of samples between hollows and hummocks. On the other hand, the highest CH_4 emission was obtained when relative elevation was at a midpoint (Figure 8B). Therefore, other factors controlling CH_4 fluxes might be important in this study site, such as hydrostatic pressure (Pelletier and others 2007; Turetsky and others 2014), increased oxidation in standing water (Strack and others 2004), and nutrient status and chemical composition of the peat (Wright and others 2011; Könönen and others 2018), especially in deeper soil profiles where CH_4 is produced.

Wong and others (2018) reported that annual CH_4 emission was 7.5–10.8 g C m^{-2} y^{-1}, which was measured above the forest canopy by the eddy covariance method in the same site as this study. The ecosystem-scale CH_4 emission was 2–3 times higher than our soil CH_4 emission (Table 3). Firstly, the soil CH_4 effluxes might miss the ebullition fluxes, because spike-like effluxes were removed as outliers through the quality control of stationarity (Table S1). Secondly, soil CH_4 is mediated by aerial roots (Adji and others 2014) and emitted from tree stems in tropical peat swamp forest (Pangala and others 2013). Furthermore, Kirschke and others (2013) reviewed that CH_4 emissions from nests of termites can account for 3.2% of globally natural CH_4 sources, and various types of termite make nests aboveground here in Maludam National Park (Vaessen and others 2011). These additional CH_4 effluxes could not be measured by the chamber method on the ground. The comparison between the chamber and eddy fluxes suggests that the

Table 3. Annual Cumulative Soil CO_2 and CH_4 Emissions (g C m^{-2} y^{-1}; mean ± 1 SD)

Year	GWL (m)	CO_2 emission			CH_4 emission			
		Non-trenched (R_S, n = 10)	Non-trenched (R_S, n = 9)*	Trenched (R_H, n = 6)	Non-trenched (n = 10)	Non-trenched (n = 9)*	Trenched (n = 6)	Whole (n = 16)
2015/16	0.01 ± 0.09	872 ± 560	907 ± 582	809 ± 427	4.08 ± 3.74	4.48 ± 3.73	3.41 ± 2.11	3.95 ± 3.54
2016/17	− 0.01 ± 0.07	981 ± 683	1032 ± 704	973 ± 548	3.76 ± 4.32	4.15 ± 4.39	2.20 ± 1.21	3.27 ± 3.77
Simple ave.	0.00 ± 0.08	926 ± 610	969 ± 630	891 ± 476	3.92 ± 3.94	4.32 ± 3.95	2.80 ± 1.76	3.61 ± 3.61
Spatial ave.	− 0.01 ± 0.02	1112 ± 310		920 ± 306				2.46 ± 0.87

R_S: soil respiration.
R_H: heterotrophic respiration.
**An outlier is excluded.*
Spatial ave. represents mean of CO_2 and CH_4 emissions of Figure 9.

aboveground emissions contributed more to the total ecosystem CH_4 emission in this site.

Comparison with Previous Studies

The annual R_S (Table 3) were lower than previous studies (990–4200 g C m^{-2} y^{-1}) in tropical peatland (Inubushi and others 2003; Hirano and others 2009; Jauhiainen and others 2012; Sundari and others 2012; Melling and others 2013; Dariah and others 2014; Husnain and others 2014; Wakhid and others 2017; Ishikura and others 2018) except for 264 g C m^{-2} y^{-1} measured in a lowland paddy (Furukawa and others 2005). The R_S was significantly promoted by lower GWL (Figure 10A), suggesting that the lower R_S was partly due to the higher GWL in this site.

The annual R_H (Table 3) was within the range of 478–993 g C m^{-2} y^{-1} measured in other tropical peat swamp forest (Melling and others 2013; Jauhiainen and others 2014; Itoh and others 2017) and the range of 372–3784 g C m^{-2} y^{-1} measured in other disturbed tropical peatlands (Jauhiainen and others 2012; Melling and others 2013; Dariah and others 2014; Hirano and others 2014; Husnain and others 2014; Jauhiainen and others 2014; Itoh and others 2017; Wakhid and others 2017; Ishikura and others 2018). The R_H was also significantly promoted by lower GWL (Figure 10B), but the R_H was not low compared to other R_H with similar annual mean GWL. The R_H in this study might be overestimated by the remaining trenched roots as discussed above. Furthermore, the R_H included litter decomposition as well as oxidative peat decomposition, whereas the previous studies excluded litter during the measurement except for several studies (Jauhiainen and others 2012, 2014; Melling and others 2013). Sjögersten and others (2014) reviewed that annual litter fall is 333 ± 96 g C m^{-2} y^{-1} in tropical peat swamp forests located in Brazil, Africa, and Southeast Asia. If a steady state is assumed for litter fall and decomposition, litter fall in a year balanced with the total litter decomposition. The study site has been declared as a national park and has been under total protection for 17 years; therefore, a steady state could have been achieved. If C leaching from litter accumulation and litter fractionization are negligible, the maximum litter decomposition can be estimated to be 333 g C m^{-2} y^{-1}, which accounts for 34% of simple mean R_S and 37% of simple mean R_H. As a result, the difference between the simple mean R_H of 891 g C m^{-2} y^{-1} and the litter decomposition could be a rough estimate of annual peat decomposition (558 g C m^{-2} y^{-1}) albeit with large uncertainties.

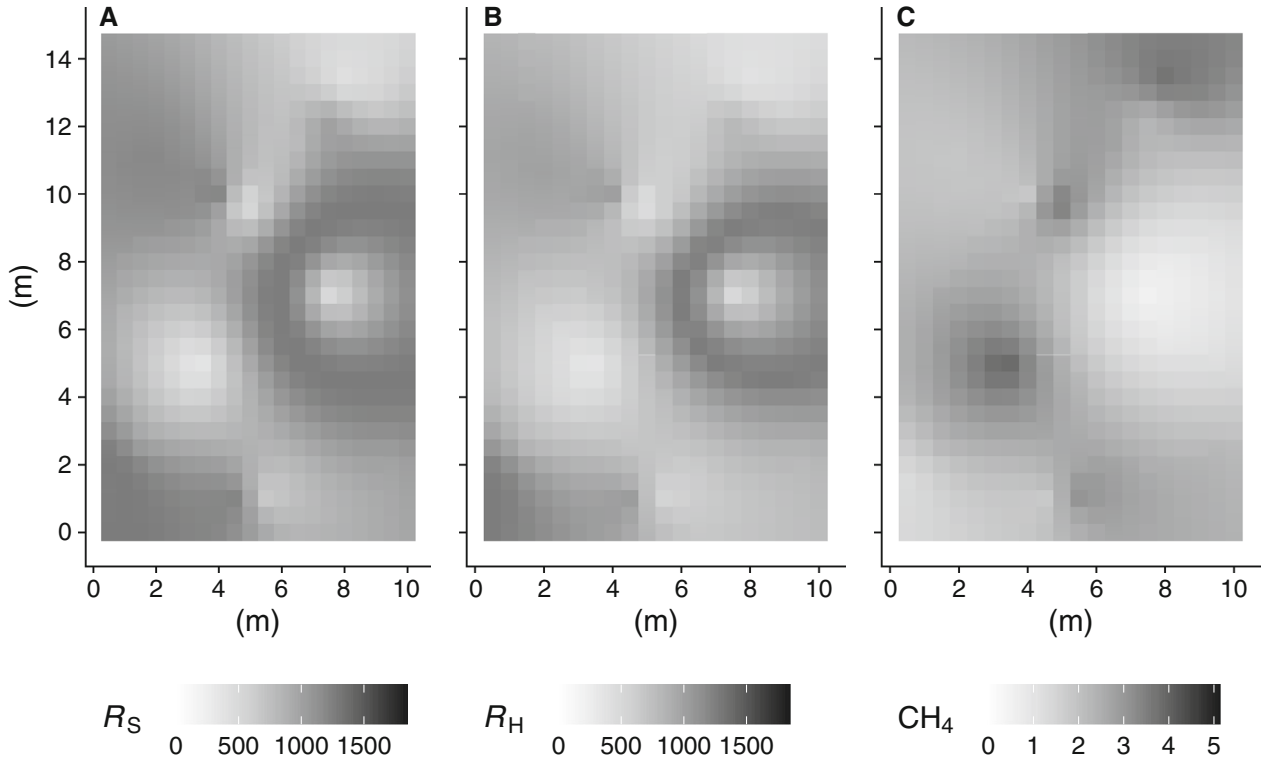

Figure 9. Spatial patterns of 2-years mean annual **A** R_S, **B** R_H, and **C** CH_4 emissions (g C m^{-2} y^{-1}).

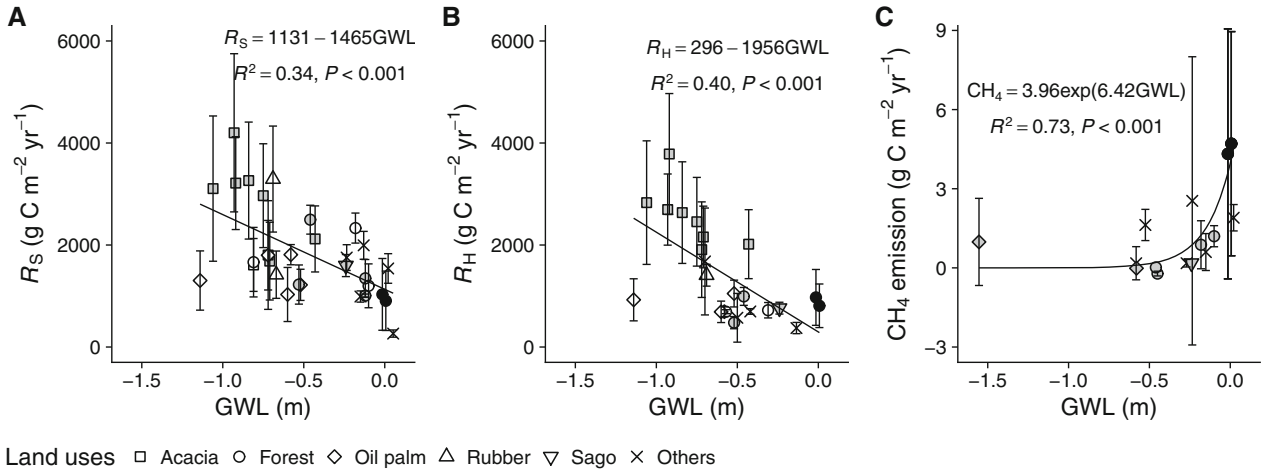

Figure 10. **A** relationship between R_S (soil respiration) and GWL (groundwater level); **B** relationship between R_H and GWL; and **C** relationship between soil CH_4 emission and GWL in the literature of tropical peatland. Error bars represent standard deviation. Black circles represent this study, gray closed symbols represent literature with litter decomposition, and open symbols represent literature without litter decomposition, respectively.

The annual soil CH_4 emission (Table 3) lay at around the high end of reported values in Southeast Asian peatland (Inubushi and others 2003; Furukawa and others 2005; Melling and others 2005a; Jauhiainen and others 2008; Hadi and others 2012). The higher soil CH_4 emission in this study mainly resulted from the higher GWL than in the previous studies (Figure 10C). In addition, the higher soil CH_4 emission could be partly attributed to the clear diurnal variation in soil CH_4 efflux (Figure 3B). In the previous studies using manual chambers, CH_4 flux was measured only in the daytime, which could have resulted in an underestimation for the cumulative emissions.

Conclusion

Soil CO_2 and CH_4 fluxes were continuously measured using an automated chamber system in an undrained tropical peat swamp forest. The soil CO_2 and CH_4 fluxes showed an unexpected diurnal variation with lower values during the daytime. The diurnal pattern may be due to the mass flow of soil gas due to thermal convection in the nighttime and atmospheric turbulence in the daytime. Decreased efflux in the daytime is expected to occur especially in closed chamber on porous peat. Thus, the chamber method may potentially underestimate CO_2 and CH_4 effluxes from peat soils, even when they are measured continuously. If a manual chamber system is applied only during the daytime like in many previous studies, more CO_2 and CH_4 emissions will be underestimated (Ishikura and others 2018). The large discrepancy in annual CH_4 emission arising from previous studies would partly be attributable to such an underestimation. On porous soils such as peat, fluxes of traces gases should be measured continuously.

The daily mean soil CO_2 and CH_4 fluxes were both controlled by GWL at the seasonal and annual scale. In this study, soil CO_2 emission was lower and CH_4 emission was higher than those in previous study, because their GWLs were lowered by drainage. Moreover, both the soil CO_2 and CH_4 emissions were controlled by relative peat surface elevation. Soil CH_4 emission might be overestimated if chambers were mainly set in hollows. Therefore, to reduce the bias, it is important to measure soil CO_2 and CH_4 emissions considering the proportion of area in hollows and hummocks equally.

Acknowledgements

The authors would like to thank the staffs in Sarawak Tropical Peat Research Institute (TROPI) for their support during the study and Shun-ichi Nakatsubo at Institute of Low Temperature Science, Hokkaido University, for chamber preparation. Malaysian Meteorological Department (Sarawak branch) and Department of Irrigation and Drainage, Sarawak supported us to provide the meteorological data. This study was supported by the Sarawak State Government and was carried out under the Joint Research Program of the Institute of Low Temperature Science, Hokkaido University. Also, this study was financially supported by JSPS KAKENHI (no. 25257401), the Environment Re-

search and Technology Development Fund (no. 2-1504) by the Environmental Restoration and Conservation Agency and the Ministry of the Environment, Japan, the Asahi Glass Foundation, and Grant for Environmental Research Projects from The Sumitomo Foundation. Moreover, this study was also partially supported by the National Institute for Environmental Studies (NIES) Internal Call for Research Proposals (A) of 2017 (Comprehensive evaluation of CH_4 and N_2O release from oil palm plantation and development of its reduction technique).

REFERENCES

Adji FF, Hamada Y, Darung U, Limin SH, Hatano R. 2014. Effect of plant-mediated oxygen supply and drainage on greenhouse gas emission from a tropical peatland in Central Kalimantan, Indonesia. Soil Sci Plant Nutr 60:1–15.

Aguilos M, Takagi K, Liang N, Watanabe Y, Teramoto M, Goto S, Takahashi Y, Mukai H, Sasa K. 2013. Sustained large stimulation of soil heterotrophic respiration rate and its temperature sensitivity by soil warming in a cool-temperate forested peatland. Tellus 65B:1–13.

Arai H, Hadi A, Darung U, Limin SH, Takahashi H, Hatano R, Inubushi K. 2014. Land use change affects microbial biomass and fluxes of carbon dioxide and nitrous oxide in tropical peatlands. Soil Sci Plant Nutr 60:423–34.

Bates D, Machler M, Bolker B, Walker S. 2015. Fitting linear mixed-effects models using lme4. J Stat Softw 67:1–48.

Birch HF. 1958. The effect of soil drying on humus decomposition and nitrogen availability. Plant Soil 10:9–31.

Borken W, Matzner E. 2009. Reappraisal of drying and wetting effects on C and N mineralization and fluxes in soils. Glob Chang Biol 15:808–24.

Bowling DR, Grote EE, Belnap J. 2011. Rain pulse response of soil CO_2 exchange by biological soil crusts and grasslands of the semiarid Colorado Plateau, United States. J Geophys Res Biogeosci 116:1–17.

Chang CP, Wang Z, McBride J, Liu CH. 2005. Annual cycle of Southeast Asia—maritime continent rainfall and the asymmetric monsoon transition. J Clim 18:287–301.

Comeau L-P, Hergoualc K, Hartill J, Smith J, Verchot LV, Peak D, Mohammad A. 2016. How do the heterotrophic and the total soil respiration of an oil palm plantation on peat respond to nitrogen fertilizer application? Geoderma 268:41–51.

Dargie GC, Lewis SL, Lawson IT, Mitchard ETA, Page SE, Bocko YE, Ifo SA. 2017. Age, extent and carbon storage of the central Congo Basin peatland complex. Nature 542:86–90.

Dariah A, Marwanto S, Agus F. 2014. Root- and peat-based CO_2 emissions from oil palm plantations. Mitig Adapt Strat Glob Change 19:831–43.

Dise NB, Gorham E, Verry ES. 1993. Environmental factors controlling methane emissions from peatlands in northern Minnesota. J Geophys Res Atmos 98:10583–94.

Dommain R, Couwenberg J, Glaser PH, Joosten H, Suryadiputra INN. 2014. Carbon storage and release in Indonesian peatlands since the last deglaciation. Quat Sci Rev 97:1–32.

Fraser FC, Corstanje R, Deeks LK, Harris JA, Pawlett M, Todman LC, Whitmore AP, Ritz K. 2016. On the origin of carbon dioxide released from rewetted soils. Soil Biol Biochem 101:1–5.

Furukawa Y, Inubushi K, Ali M, Itang AM, Tsuruta H. 2005. Effect of changing groundwater levels caused by land-use changes on greenhouse gas fluxes from tropical peat lands. Nutr Cycl Agroecosyst 71:81–91.

Ganot Y, Dragila MI, Weisbrod N. 2014. Impact of thermal convection on CO_2 flux across the earth-atmosphere boundary in high-permeability soils. Agric For Meteorol 184:12–24.

Girkin NT, Turner BL, Ostle N, Craigon J, Sjögersten S. 2018. Root exudate analogues accelerate CO_2 and CH_4 production in tropical peat. Soil Biol Biochem 117:48–55.

Görres C-M, Kammann C, Ceulemans R. 2016. Automation of soil flux chamber measurements: potentials and pitfalls. Biogeosciences 13:1949–66.

Hadi A, Fatah L, Syaifuddin Abdullah, Affandi DN, Bakar RA, Inubushi K. 2012. Greenhouse gas emissions from peat soils cultivated to rice field, oil palm and vegetable. J Trop Soils 17:105–14.

Hadi A, Inubushi K, Furukawa Y, Purnomo E, Rasmadi M, Tsuruta H. 2005. Greenhouse gas emissions from tropical peatlands of Kalimantan, Indonesia. Nutr Cycl Agroecosyst 71:73–80.

Hanson PJ, Edwards NT, Garten CT, Andrews JA. 2000. Separating root and soil microbial contributions to soil respiration: a review of methods and observations. Biogeochemistry 48:115–46.

Harazono Y, Iwata H, Sakabe A, Ueyama M, Takahashi K, Nagano H, Nakai T, Kosugi Y. 2015. Effects of water vapor dilution on trace gas flux, and practical correction methods. J Agric Meteorol 71:65–76.

He X, Inoue T. 2015. Peatland Tank Model for evaluation of shallow groundwater table data without height reference from benchmark. Int J Environ Rural Dev 6:16–21.

Hirano T, Jauhiainen J, Inoue T, Takahashi H. 2009. Controls on the carbon balance of tropical peatlands. Ecosystems 12:873–87.

Hirano T, Kusin K, Limin S, Osaki M. 2014. Carbon dioxide emissions through oxidative peat decomposition on a burnt tropical peatland. Glob Chang Biol 20:555–65.

Husnain H, Wigena IGP, Dariah A, Marwanto S, Setyanto P, Agus F. 2014. CO_2 emissions from tropical drained peat in Sumatra, Indonesia. Mitig Adapt Strat Glob Change 19:845–62.

Huxman T, Snyder K, Tissue D, Leffler AJ, Ogle K, Pockman W, Sandquist D, Potts D, Schwinning S. 2004. Precipitation pulses and carbon fluxes in semiarid and arid ecosystems. Oecologia 141:254–68.

Inubushi K, Furukawa Y, Hadi A, Purnomo E, Tsuruta H. 2003. Seasonal changes of CO_2, CH_4 and N_2O fluxes in relation to land-use change in tropical peatlands located in coastal area of South Kalimantan. Chemosphere 52:603–8.

IPCC. 2013. Climate Change 2013: The Physical Science Basis. Contribution of Working Group I to the Fifth Assessment Report of the Intergovernmental Panel on Climate Change. (Stocker TF, Qin D, Plattner G-K, Tignor M, Allen SK, Boschung J, Nauels A, Xia Y, Bex V, Midgley PM, editors.). Cambridge, United Kingdom and New York, NY, USA: Cambridge University Press

Ishikura K, Hirano T, Okimoto Y, Hirata R, Kiew F, Melling L, Aeries EB, Lo KS, Musin KK, Waili JW, Wong GX, Ishii Y. 2018. Soil carbon dioxide emissions due to oxidative peat

decomposition in an oil palm plantation on tropical peat. Agric Ecosyst Environ 254:202–12.

Ishikura K, Yamada H, Toma Y, Takakai F, Morishita T, Darung U, Limin A, Limin SH, Hatano R. 2017. Effect of groundwater level fluctuation on soil respiration rate of tropical peatland in Central Kalimantan, Indonesia. Soil Sci Plant Nutr 63:1–13.

Itoh M, Okimoto Y, Hirano T, Kusin K. 2017. Factors affecting oxidative peat decomposition due to land use in tropical peat swamp forests in Indonesia. Sci Total Environ 609:906–15.

IUSS Working Group WRB. 2015. World Reference Base for Soil Resources 2014, update 2015 International soil classification system for naming soils and creating legends for soil maps. Rome: World Soil Resources Reports No. 106. FAO

Jassal RS, Black TA, Nesic Z, Gaumont-Guay D. 2012. Using automated non-steady-state chamber systems for making continuous long-term measurements of soil CO_2 efflux in forest ecosystems. Agric For Meteorol 161:57–65.

Jauhiainen J, Hooijer A, Page SE. 2012. Carbon dioxide emissions from an *Acacia* plantation on peatland in Sumatra, Indonesia. Biogeosciences 9:617–30.

Jauhiainen J, Kerojoki O, Silvennoinen H, Limin S, Vasander H. 2014. Heterotrophic respiration in drained tropical peat is greatly affected by temperature—a passive ecosystem cooling experiment. Environ Res Lett 9:105013.

Jauhiainen J, Limin S, Silvennoinen H, Vasander H. 2008. Carbon dioxide and methane fluxes in drained tropical peat before and after hydrological restoration. Ecology 89:3503–14.

Kamewada K. 1997. Cation exchange capacity (semi-micro Schollenberger method). In: Editorial Committee of Methods of Soil Environment Analysis, editor. Methods of Soil Environment Analysis. Tokyo: Hakuyu-sha. pp 208–11.

Kiew F, Hirata R, Hirano T, Wong GX, Aeries EB, Musin KK, Waili JW, Lo KS, Shimizu M, Melling L. 2018. CO_2 balance of a secondary tropical peat swamp forest in Sarawak, Malaysia. Agric For Meteorol 248:494–501.

Kirschke S, Bousquet P, Ciais P, Saunois M, Canadell JG, Dlugokencky EJ, Bergamaschi P, Bergmann D, Blake DR, Bruhwiler L, Cameron-Smith P, Castaldi S, Chevallier F, Feng L, Fraser A, Heimann M, Hodson EL, Houweling S, Josse B, Fraser PJ, Krummel PB, Lamarque J-F, Langenfelds RL, Le Quéré C, Naik V, O'Doherty S, Palmer PI, Pison I, Plummer D, Poulter B, Prinn RG, Rigby M, Ringeval B, Santini M, Schmidt M, Shindell DT, Simpson IJ, Spahni R, Steele LP, Strode SA, Sudo K, Szopa S, van der Werf GR, Voulgarakis A, van Weele M, Weiss RF, Williams JE, Zeng G. 2013. Three decades of global methane sources and sinks. Nat Geosci 6:813–23.

Könönen M, Jauhiainen J, Straková P, Heinonsalo J, Laiho R, Kusin K, Limin S, Vasander H. 2018. Deforested and drained tropical peatland sites show poorer peat substrate quality and lower microbial biomass and activity than unmanaged swamp forest. Soil Biol Biochem 123:229–41.

Lai DYF, Roulet NT, Humphreys ER, Moore TR, Dalva M. 2012. The effect of atmospheric turbulence and chamber deployment period on autochamber CO_2 and CH_4 flux measurements in an ombrotrophic peatland. Biogeosciences 9:3305–22.

Lampela M, Jauhiainen J, Vasander H. 2014. Surface peat structure and chemistry in a tropical peat swamp forest. Plant Soil 382:329–47.

Lawson IT, Kelly TJ, Aplin P, Boom A, Dargie G, Draper FCH, Hassan PNZBP, Hoyos-Santillan J, Kaduk J, Large D, Murphy W, Page SE, Roucoux KH, Sjögersten S, Tansey K, Waldram M, Wedeux BMM, Wheeler J. 2014. Improving estimates of tropical peatland area, carbon storage, and greenhouse gas fluxes. Wetl Ecol Manag 23:327–46.

Marumoto T, Kai H, Yoshida T, Harada T. 1977. Drying effect on mineralizations of microbial cells and their cell walls in soil and contribution of microbial cell walls as a source of decomposable soil organic matter due to drying. Soil Sci Plant Nutr 23:9–19.

Melling L. 2016. Peatland in Malaysia. In: Osaki M, Tsuji N, Eds. Tropical peatland ecosystems. Springer Japan: Tokyo. p 59–73.

Melling L, Hatano R, Goh KJ. 2005a. Methane fluxes from three ecosystems in tropical peatland of Sarawak, Malaysia. Soil Biol Biochem 37:1445–53.

Melling L, Hatano R, Goh KJ. 2005b. Soil CO_2 flux from three ecosystems in tropical peatland of Sarawak, Malaysia. Tellus 57B:1–11.

Melling L, Yun Tan CS, Goh KJ, Hatano R. 2013. Soil microbial and root respirations from three ecosystems in tropical peatland of Sarawak, Malaysia. J Oil Palm Res 25:44–57.

Miettinen J, Hooijer A, Vernimmen R, Liew SC, Page SE. 2017. From carbon sink to carbon source: extensive peat oxidation in insular Southeast Asia since 1990. Environ Res Lett 12:024014.

Minamikawa K, Sakai N. 2006. The practical use of water management based on soil redox potential for decreasing methane emission from a paddy field in Japan. Agric Ecosyst Environ 116:181–8.

Murakami M, Furukawa Y, Inubushi K. 2005. Methane production after liming to tropical acid peat soil. Soil Sci Plant Nutr 51:697–9.

Olefeldt D, Turetsky MR, Crill PM, Mcguire AD. 2013. Environmental and physical controls on northern terrestrial methane emissions across permafrost zones. Glob Chang Biol 19:589–603.

Page SE, Rieley JO, Banks CJ. 2011. Global and regional importance of the tropical peatland carbon pool. Glob Chang Biol 17:798–818.

Page SE, Wust RAJ, Weiss D, Rieley JO, Shotyk W, Limin SH. 2004. A record of Late Pleistocene and Holocene carbon accumulation and climate change from an equatorial peat bog (Kalimantan, Indonesia): implications for past, present and future carbon dynamics. J Quat Sci 19:625–35.

Pangala SR, Moore S, Hornibrook ERC, Gauci V. 2013. Trees are major conduits for methane egress from tropical forested wetlands. New Phytol 197:524–31.

Pelletier L, Moore TR, Roulet NT, Garneau M, Beaulieu-Audy V. 2007. Methane fluxes from three peatlands in the La Grande Rivière watershed, James Bay lowland, Canada. J Geophys Res 112:G01018. https://doi.org/10.1029/2006JG000216.

Placella SA, Brodie EL, Firestone MK. 2012. Rainfall-induced carbon dioxide pulses result from sequential resuscitation of phylogenetically clustered microbial groups. Proc Natl Acad Sci 109:10931–6.

Poindexter CM, Variano EA. 2013. Gas exchange in wetlands with emergent vegetation: The effects of wind and thermal convection at the air–water interface. J Geophys Res Biogeosci 118:1297–306.

R Core Team. 2017. R: A Language and Environment for Statistical Computing. Vienna, Austria: R Foundation for Statistical Computing. https://www.r-project.org/

Sakabe A, Itoh M, Hirano T, Kusin K. 2018. Ecosystem-scale methane flux in tropical peat swamp forest in Indonesia. Glob Chang Biol 24(11):5123–36.

Sangok FE, Maie N, Melling L, Watanabe A. 2017. Evaluation on the decomposability of tropical forest peat soils after conversion to an oil palm plantation. Sci Total Environ 587–588:381–8.

Sjögersten S, Black CR, Evers S, Hoyos-Santillan J, Wright EL, Turner BL. 2014. Tropical wetlands: a missing link in the global carbon cycle? Global Biogeochem Cycles 28:1371–86.

Sjögersten S, Cheesman AW, Lopez O, Turner BL. 2011. Biogeochemical processes along a nutrient gradient in a tropical ombrotrophic peatland. Biogeochemistry 104:147–63.

Smith LC, MacDonald GM, Velichko AA, Beilman DW, Borisova OK, Frey KE, Kremenetski KV, Sheng Y. 2004. Siberian peatlands a net carbon sink and global methane source since the early Holocene. Science 303:353–6.

Strack M, Waddington JM, Tuittila E-S. 2004. Effect of water table drawdown on peatland nutrient dynamics: Implications for climate change. Biogeochemistry 18:661–76.

Sundari S, Hirano T, Yamada H, Kusin K, Limin S. 2012. Effect of groundwater level on soil respiration in tropical peat swamp forests. J Agric Meteorol 68:121–34.

Susilawati HL, Setyanto P, Ariani M, Hervani A, Inubushi K. 2016. Influence of water depth and soil amelioration on greenhouse gas emissions from peat soil columns. Soil Sci Plant Nutr 62:57–68.

Teh YA, Murphy WA, Berrio J, Boom A, Page SE. 2017. Seasonal variability in methane and nitrous oxide fluxes from tropical peatlands in the western Amazon basin. Biogeosciences 14:3669–83.

Toma Y, Takakai F, Darung U, Kuramochi K, Limin SH, Dohong S, Hatano R. 2011. Nitrous oxide emission derived from soil organic matter decomposition from tropical agricultural peat soil in central Kalimantan, Indonesia. Soil Sci Plant Nutr 57:436–51.

Turetsky MR, Kotowska A, Bubier J, Dise NB, Crill P, Hornibrook ERC, Minkkinen K, Moore TR, Myers-Smith IH, Nykänen H, Olefeldt D, Rinne J, Saarnio S, Shurpali N, Tuittila ES, Waddington JM, White JR, Wickland KP, Wilmking M. 2014. A synthesis of methane emissions from 71 northern, temperate, and subtropical wetlands. Glob Chang Biol 20:2183–97.

Vaessen T, Verwer C, Demies M, Kaliang H, Van Der Meer PJ. 2011. Comparison of termite assemblages along a landuse gradient on peat areas in Sarawak, Malaysia. J Trop For Sci 23:196–203.

Wakhid N, Hirano T, Okimoto Y, Nurzakiah S, Nursyamsi D. 2017. Soil carbon dioxide emissions from a rubber plantation on tropical peat. Sci Total Environ 581–582:857–65.

Wong GX, Hirata R, Hirano T, Kiew F, Aeries EB, Musin KK, Waili JW, Lo KS, Melling L. 2018. Micrometeorological measurement of methane flux above a tropical peat swamp forest. Agric For Meteorol 256–257:353–61.

Wright EL, Black CR, Cheesman AW, Drage T, Large D, Turner BL, Sjögersten S. 2011. Contribution of subsurface peat to CO_2 and CH_4 fluxes in a neotropical peatland. Glob Chang Biol 17:2867–81.

Wright EL, Black CR, Turner BL, Sjögersten S. 2013. Environmental controls of temporal and spatial variability in CO_2 and CH_4 fluxes in a neotropical peatland. Glob Chang Biol 19:3775–89.

Yagi K, Tsuruta H, Kanda K-I, Minami K. 1996. Effect of water managment on methane emission from a Japanese rice paddy field: Automated methane monitoring. Global Biogeochem Cycles 10:255–67.

Yu Z, Loisel J, Brosseau DP, Beilman DW, Hunt SJ. 2010. Global peatland dynamics since the Last Glacial Maximum. Geophys Res Lett 37:L13402.